A commentary by Linda A. Dahlgren, DVM, PhD, DACVS, is linked to the online version of this article at jbjs.org.

Addition of Mesenchymal Stem Cells to Autologous Platelet-Enhanced Fibrin Scaffolds in Chondral Defects

Does It Enhance Repair?

Laurie R. Goodrich, DVM, PhD, Albert C. Chen, PhD, Natasha M. Werpy, DVM, Ashley A. Williams, MS, John D. Kisiday, PhD, Alvin W. Su, MD, PhD, Esther Cory, MA, Paul S. Morley, DVM, PhD, C. Wayne McIlwraith, BVSc, PhD, DSc, FRCVS, Robert L. Sah, MD, ScD, and Constance R. Chu, MD

Investigation performed at the Gail Holmes Equine Orthopedic Research Center, Colorado State University, Fort Collins, Colorado; Stanford University, Stanford, California; University of Pittsburgh, Pittsburgh, Pennsylvania; and University of California, San Diego, La Jolla, California

Background: The chondrogenic potential of culture-expanded bone-marrow-derived mesenchymal stem cells (BMDMSCs) is well described. Numerous studies have also shown enhanced repair when BMDMSCs, scaffolds, and growth factors are placed into chondral defects. Platelets provide a rich milieu of growth factors and, along with fibrin, are readily available for clinical use. The objective of this study was to determine if the addition of BMDMSCs to an autologous platelet-enriched fibrin (APEF) scaffold enhances chondral repair compared with APEF alone.

Methods: A 15-mm-diameter full-thickness chondral defect was created on the lateral trochlear ridge of both stifle joints of twelve adult horses. In each animal, one defect was randomly assigned to receive APEF+BMDMSCs and the contralateral defect received APEF alone. Repair tissues were evaluated one year later with arthroscopy, histological examination, magnetic resonance imaging (MRI), micro-computed tomography (micro-CT), and biomechanical testing.

Results: The arthroscopic findings, MRI T2 map, histological scores, structural stiffness, and material stiffness were similar ($p > 0.05$) between the APEF and APEF+BMDMSC-treated repairs at one year. Ectopic bone was observed within the repair tissue in four of twelve APEF+BMDMSC-treated defects. Defects repaired with APEF alone had less trabecular bone edema (as seen on MRI) compared with defects repaired with APEF+BMDMSCs. Micro-CT analysis showed thinner repair tissue in defects repaired with APEF+BMDMSCs than in those treated with APEF alone ($p < 0.05$).

Conclusions: APEF alone resulted in thicker repair tissue than was seen with APEF+BMDMSCs. The addition of BMDMSCs to APEF did not enhance cartilage repair and stimulated bone formation in some cartilage defects.

Clinical Relevance: APEF supported repair of critical-size full-thickness chondral defects in horses, which was not improved by the addition of BMDMSCs. This work supports further investigation to determine whether APEF enhances cartilage repair in humans.

Peer Review: This article was reviewed by the Editor-in-Chief and one Deputy Editor, and it underwent blinded review by two or more outside experts. The Deputy Editor reviewed each revision of the article, and it underwent a final review by the Editor-in-Chief prior to publication. Final corrections and clarifications occurred during one or more exchanges between the author(s) and copyeditors.

Repair of full-thickness articular cartilage defects continues to challenge orthopaedic surgeons. Microfracture is a first-line treatment for smaller defects, although mesenchymal stem cell transplantation has been evaluated for larger defects in animal and human studies[1-4]. Investigators have used culture-expanded cells or same-day implantation of bone marrow aspirate

Disclosure: One or more of the authors received payments or services, either directly or indirectly (i.e., via his or her institution), from a third party in support of an aspect of this work. In addition, one or more of the authors, or his or her institution, has had a financial relationship, in the thirty-six months prior to submission of this work, with an entity in the biomedical arena that could be perceived to influence or have the potential to influence what is written in this work. No author has had any other relationships, or has engaged in any other activities, that could be perceived to influence or have the potential to influence what is written in this work. The complete **Disclosures of Potential Conflicts of Interest** submitted by authors are always provided with the online version of the article.

TABLE I Arthroscopic (ICRS) Grading of Cartilage Repair*

	Points
Degree of defect repair	
Level with surrounding cartilage	4
75% of defect depth	3
50% of defect depth	2
25% of defect depth	1
0% of defect depth	0
Integration to border zone	
Complete integration with surrounding cartilage	4
Demarcating border <1 mm	3
3/4 of graft integrated with surrounding cartilage, 1/4 with notable border of >1 mm	2
1/2 of graft integrated with surrounding cartilage, 1/2 with notable border of >1 mm	1
From no contact to 1/4 of graft integrated with surrounding cartilage	0
Macroscopic appearance	
Intact smooth surface	4
Fibrillated surface	3
Small, scattered fissures or cracks	2
Several small or few but large fissures	1
Total degeneration of grafted area	0
Overall repair assessment	
Grade I: normal	12
Grade II: nearly normal	8-11
Grade III: abnormal	4-7
Grade IV: severely abnormal	1-3

*The maximum possible score is 12 points, and a higher score is better.

TABLE II MRI Scoring System for Subchondral Bone*

	Points
Subchondral bone density: abnormal signal intensity in the subchondral bone deep to the defect indicating a loss in density	
0% (none)	0
1%-25% (slight)	1
26%-50% (mild)	2
51%-75% (moderate)	3
76%-100% (severe)	4
Subchondral bone fluid/edema; distribution and size of affected area also considered	
0% (none)	0
1%-25% (slight)	1
26%-50% (mild)	2
51%-75% (moderate)	3
76%-100%—include cystic change (severe)	4
Trabecular bone sclerosis as compared with the normal signal pattern for trabecular bone versus subchondral bone (guide for dense bone with no fat); distribution and size of affected area also considered	
0% (none)	0
1%-25% (slight)	1
26%-50% (mild)	2
51%-75% (moderate)	3
76%-100% (severe)	4
Trabecular bone edema as compared with the signal intensity of synovial fluid representing the fluid content in the bone; distribution and size of affected area also considered	
0% (none)	0
1%-25% (slight)	1
26%-50% (mild)	2
51%-75% (moderate)	3
76%-100% (severe)	4
Subchondral bone overgrowth as proportion of defect depth; area affected also considered	
0% (none)	0
1%-25% (slight)	1
26%-50% (mild)	2
51%-75% (moderate)	3
76%-100% (marked)	4

*The maximum possible score is 20 points, and a lower score is better.

concentrate[2,5-9]. Tens of millions of cells may be necessary to enhance the accumulation of cartilage-like matrix[10], which suggests that culture expansion may be imperative to attain suitable outcomes. In a recent review of stem cell therapies for cartilage defects, it was reported that culture-expanded bone-marrow-derived mesenchymal stem cells (BMDMSCs) had been implanted in nine of eleven clinical studies[11]. Although some of the reports suggested beneficial results, to our knowledge no randomized controlled studies of humans have been performed to show whether implantation of BMDMSCs in chondral defects enhances outcomes.

While stem cell therapy for cartilage repair holds promise, combining BMDMSCs with additional biologics such as platelet-rich plasma may further stimulate healing[4,12-14]. This milieu of growth factors may enhance cell viability, migration, and chondrogenic differentiation. It may also negate detrimental effects of catabolic cytokines (such as interleukin [IL]-1β derived from an inflamed joint) on cartilage[15]. In several clinical case series, a combination of platelet-rich plasma and BMDMSCs were implanted in osteochondral defects with somewhat promising results; however, to our knowledge there have been no efforts to

TABLE III MRI Scoring System for Fill of Chondral Defect*

	Points
Amount of defect fill: percentage of defect filled as compared with the signal intensity of normal articular cartilage; interface not included	
0% (none)	0
1%-25% (slight)	1
26%-50% (mild)	2
51%-75% (moderate)	3
76%-100% (marked to complete)	4
Character of defect fill as compared with the signal intensity of normal articular cartilage; interface not included	
0% (none)	0
1%-25% (slight)	1
26%-50% (mild)	2
51%-75% (moderate)	3
76%-100% (marked)	4
Interface of defect: overall character of the signal intensity of the tissue at the interface as compared with normal articular cartilage	
0% (none)	0
1%-25% (slight)	1
26%-50% (mild)	2
51%-75% (moderate)	3
76%-100% (marked)	4

*The maximum possible score is 12 points, and a higher score is better.

elucidate the individual contributions of each[4,16,17]. Considering the potential benefits of both culture-expanded BMDMSCs and platelet-rich plasma, our objective was to answer the question of whether BMDMSCs combined with platelet-rich plasma would enhance chondral repair and regenerate hyaline cartilage when compared with platelet-rich plasma alone. Our hypothesis was

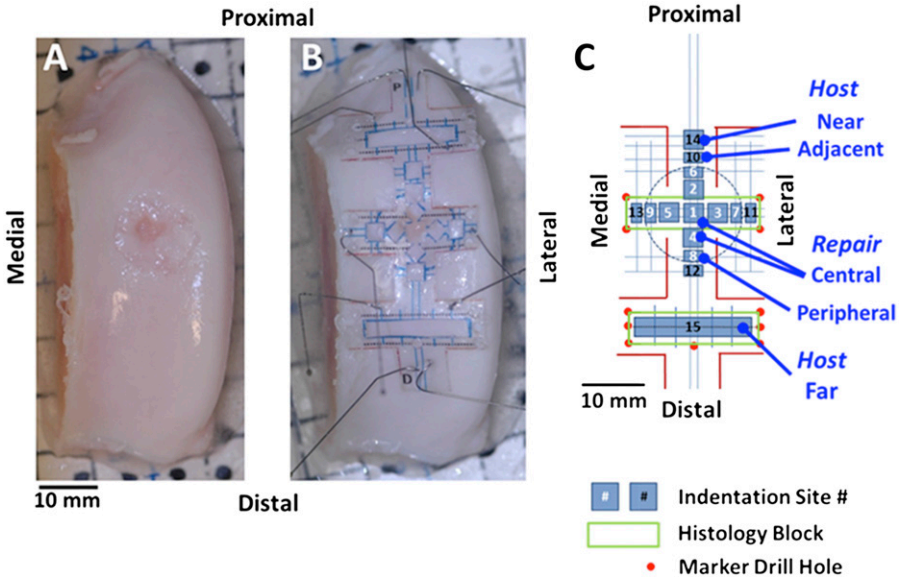

Fig. 1

At twelve months following creation of a cartilage defect and filling it with APEF or APEF+BMDMSCs, the trochleae were imaged, before (**Fig. 1-A**) and after (**Fig. 1-B**) applying a template, prior to indentation testing, micro-CT imaging, and histological analysis. In the schematic of sample sites relative to the lesion (**Fig. 1-C**), sites 1 through 5 are the central repair region, sites 6 through 9 are the peripheral repair region, sites 10 through 13 are the adjacent host region, site 14 is the near host region, and site 15 is the far host region.

TABLE IV Histological Scoring System for Repair Tissue*

	Points
Nature of predominant tissue	
Cellular morphology	
Hyaline cartilage	4
Mostly hyaline cartilage	3
Mixed hyaline and fibrocartilage	2
Mostly fibrocartilage	1
Some fibrocartilage, mostly nonchondrocytic cells	0
Safranin-O staining	
Normal or nearly normal	3
Moderate	2
Slight	1
None	0
Structural characteristics	
Surface	
Smooth and intact	3
Superficial horizontal lamination	2
Fissures	1
Severe disruption, including fibrillation	0
Structural integrity	
Normal	2
Slight disruption, including cysts	1
Severe disintegration, disruptions	0
Thickness	
100% of normal adjacent cartilage	2
50%-99% of normal adjacent cartilage	1
0%-49% of normal adjacent cartilage	0
Bonding to adjacent cartilage	
Bonded at both ends of the graft	2
Bonded at 1 end or partially at both ends	1
Not bonded	0
Reconstruction of subchondral bone	
Normal	3
Reduced	2
Minimal	1
None	0
Inflammatory response in subchondral bone region	
None/mild	2
Moderate	1
Severe	0
Degenerative changes: graft	
Hypocellularity	
Normal cellularity	2
Slight hypocellularity	1
Moderate hypocellularity or hypercellularity	0
Chondrocyte clustering	
No clusters	2
<25% of cells	1
25%-100% of cells	0
Freedom from degenerative changes in adjacent cartilage	
Normal cellularity, no clusters, normal staining	3
Normal cellularity, mild clusters, moderate staining	2
Mild/moderate cellularity, moderate clusters, moderate hypocellularity, slight staining	1
Severe hypocellularity and degeneration, poor or no staining	0

*The maximum possible score is 28 points, and a higher score is better.

that the addition of BMDMSCs to an autologous platelet-enhanced fibrin (APEF) scaffold would enhance cartilage repair compared with APEF alone when evaluated with arthroscopy, histological examination, magnetic resonance imaging (MRI), and biomechanical analysis.

Materials and Methods

For an expanded, more detailed Materials and Methods section, see the Appendix.

Horses: Physical Examinations

Twelve healthy horses between the ages of two and five years were entered into the study, and animal protocols were approved by the Colorado State University animal care and use committee.

Isolation and Expansion of BMDMSCs and Preparation of APEF

Bone marrow was aspirated from the ilium four weeks prior to surgery, and BMDMSCs were prepared as previously described[18]. The day before surgery, cells were thawed and plated. On the day of implantation, cells were trypsinized, washed, and combined with the fibrinogen portion of the fibrin glue. APEF was prepared from blood collected from each animal on the day of surgery. Blood was collected into an acid citrate dextrose (ACD) bag, and fibrinogen was prepared as previously described[19]. When the fibrinogen/platelet mixture was mixed 1:1 with the thrombin solution, the final concentration in the defect was 1 billion platelets/mL. In each horse, one defect was randomly assigned to receive approximately 1 mL of APEF+BMDMSCs (10 million cells) and the contralateral defect was treated with APEF alone.

Arthroscopic Defect Creation and Defect Grafting

A customized reamer was used to create a 15-mm-diameter round chondral defect arthroscopically on the lateral trochlear ridge of both femoropatellar joints as previously described[20]. A needle was attached to a Duploject syringe (Baxter) and positioned over the defect. APEF or APEF+BMDMSCs was delivered and allowed to polymerize[20].

Arthroscopic Examinations at Three Months After Defect Creation and Post Mortem at Twelve Months

Three months following defect creation and scaffold placement, arthroscopic examinations were performed and the defects were graded by surgeons blinded to the treatment group[20]. The horses were euthanized twelve months following defect creation. The stifles were excised and kept on ice prior to MRI analysis and

TABLE V Arthroscopic (ICRS) Scores for Cartilage Repair*

	Mean Score ± SD *(points)*	
	APEF	APEF+BMDMSCs
3 months		
Degree of defect repair	2.33 ± 0.78	3.23 ± 0.75
Integration to border zone	3.33 ± 0.89	3.45 ± 0.82
Macroscopic appearance	2.75 ± 1.06	3.73 ± 0.47
Composite score	8.40 ± 1.93	10.41 ± 1.59
1 year		
Degree of defect repair	3.25 ± 0.72	3.17 ± 0.62
Integration to border zone	2.33 ± 0.91	2.63 ± 0.86
Macroscopic appearance	2.50 ± 1.07	2.42 ± 0.70
Composite score	8.2 ± 2.08	8.25 ± 1.47

*A higher score is better.

arthroscopic examination. All defects were probed with an arthroscopic instrument, photographed, and graded by surgeons blinded to treatment group[21] (Table I).

MRI

Images were acquired using a 3-T human clinical MRI scanner (MAGNETOM Trio Tim, Siemens Medical Solutions) with an eight-channel knee coil (Invivo). Sequences used to grade defects were 3D (three-dimensional) DESS (double echo in the steady state), 3D proton density, and 2D fat-saturated proton density. All MRIs were evaluated in multiple categories by a radiologist blinded to the treatment group[22,23] (Tables II and III).

Quantitative MRI (qMRI) T2 Mapping of Equine Explants

For qMRI assessment, osteochondral explants consisting of the lateral trochlear ridge of each stifle were harvested. Axial T2-weighted images were acquired with a multi-slice multi-echo spin-echo sequence with seven echoes. Following MRI, explants were frozen for subsequent analyses. T2 maps were calculated with a mono-exponential pixel-by-pixel T2-fit routine using MRI Mapper software (Beth Israel Deaconess Medical Center and MIT [Massachusetts Institute of Technology]) running on a MATLAB platform (The MathWorks). A single axial slice from the center of each cartilage repair was evaluated.

Indentation Testing

A transparent overlay was positioned over the lesion and surrounding cartilage surface to localize sites for biomechanical tests, micro-computed tomography (micro-CT) registration marks, and histological examination (Figs. 1-A and 1-B). Cartilage load-bearing function was determined by indentation testing in

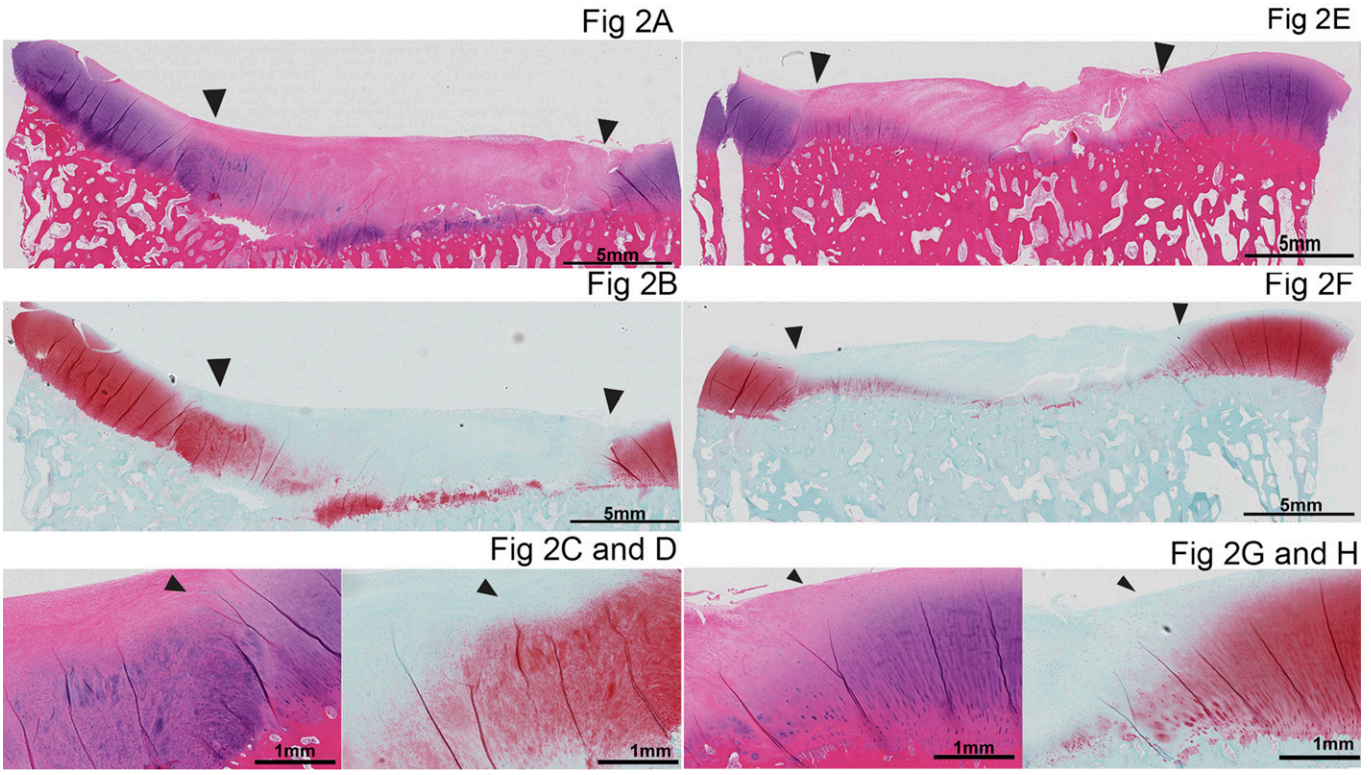

Fig. 2

Histological appearance of repair tissue from the APEF (**Figs. 2-A through 2-D**) and APEF+BMDMSCs (**Figs. 2-E through 2-H**) groups. **Figures 2-A, 2-C, 2-E, and 2-G** are stained with hematoxylin and eosin, and **Figures 2-B, 2-D, 2-F, and 2-H** are stained with safranin O. The arrowheads point to the periphery of the defect, where the repair tissue borders the surrounding peripheral tissue. The images in the bottom row are close-up photomicrographs of the integration of the repair tissue with the surrounding peripheral cartilage in the APEF group **(Figs. 2-C and 2-D)** and the APEF+BMDMSCs group (**Figs. 2-G and 2-H**).

TABLE VI Histological Scores for Repair Tissue*

	Mean Score ± SD *(points)*	
	APEF	APEF+BMDMSCs
Cellular morphology	1.25 ± 0.75	1.42 ± 0.79
Safranin-O staining	0.83 ± 0.71	1.33 ± 0.49
Surface characteristics	1.58 ± 1.24	1.83 ± 1.11
Structural integrity	0.92 ± 0.67	0.83 ± 0.58
Thickness	1.42 ± 0.67	1.08 ± 0.51
Bonding to adjacent cartilage	2.0 ± 0.0	1.83 ± 0.39
Reconstruction of subchondral bone	2.58 ± 0.52	2.17 ± 0.39
Inflammatory response in subchondral bone region	2.0 ± 0.0	2.0 ± 0.0
Degenerative changes: graft	0.67 ± 0.65	0.42 ± 0.51
Chondrocyte clustering	1.25 ± 0.75	1.25 ± 0.62
Degenerative changes in adjacent cartilage	2.83 ± 0.39	2.33 ± 0.65

*A higher score is better.

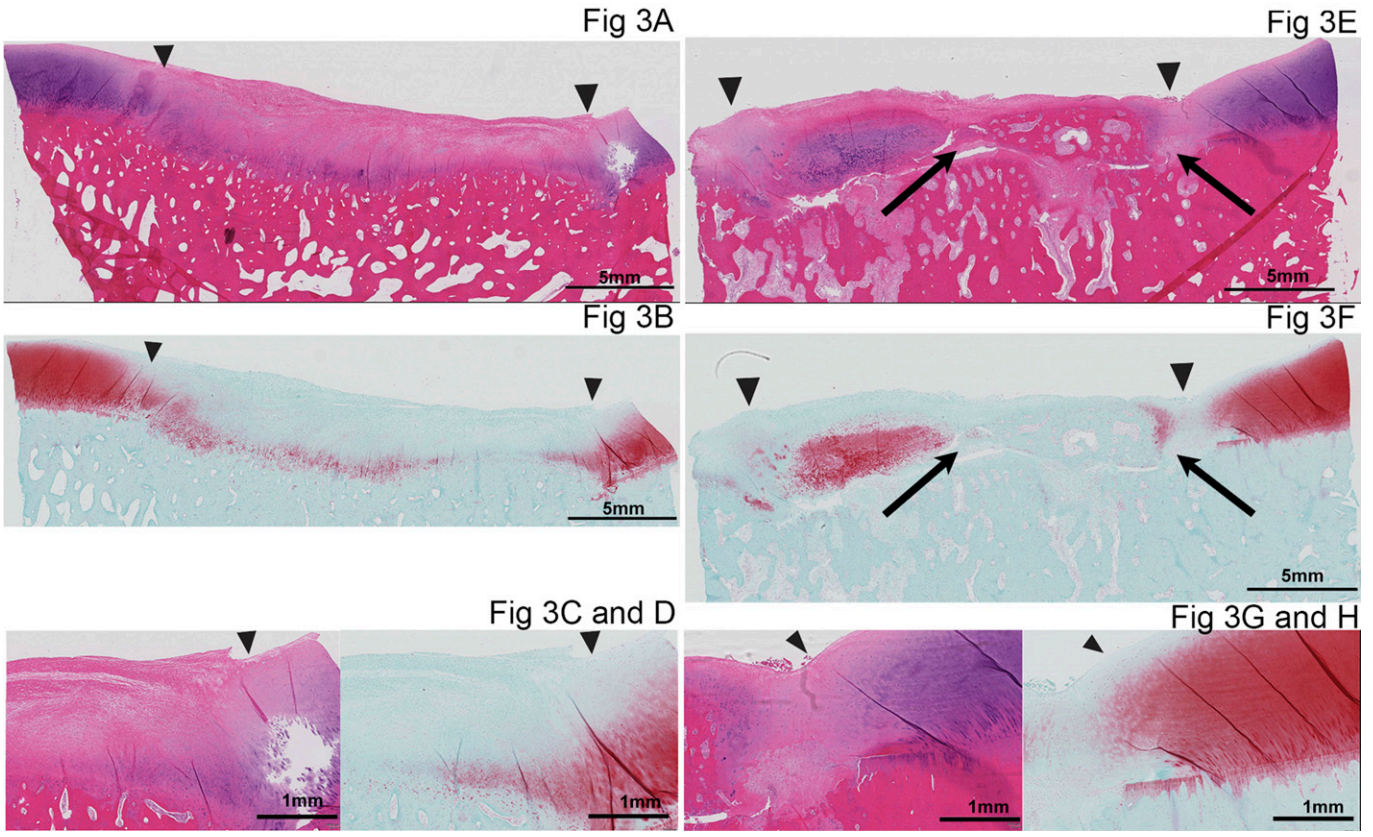

Fig. 3

Histological appearance of the defects of a horse in which bone formed within the repair tissue in the limb treated with APEF+BMDMSCs. **Figures 3-A, 3-C, 3-E, and 3-G** are stained with hematoxylin and eosin, and **Figures 3-B, 3D, 3-F, and 3-H** are stained with safranin O. The defect repaired with APEF is shown on the left (**Figs. 3-A through 3-D**) and the defect repaired with APEF+BMDMSCs is shown on the right (**Figs. 3-E through 3-H**). The arrowheads point to the periphery of the defect, where the repair tissue borders the surrounding peripheral tissue. The images in the bottom row are close-up photomicrographs of the integration of the repair tissue with the surrounding peripheral cartilage in the APEF group (**Figs. 3-C and 3-D**) and the APEF+BMDMSCs group (**Figs. 3-G and 3-H**). The defect repaired with APEF+BMDMSCs (**Figs. 3-E and 3-F**) has bone (arrows) within the repair tissue.

TABLE VII MRI Scores for Subchondral Bone*

	Mean Score ± SD *(points)*	
	APEF	APEF+BMDMSCs
Subchondral bone density	2.45 ± 0.82	2.91 ± 0.83
Subchondral bone fluid/edema	2.0 ± 0.77	2.46 ± 1.04
Trabecular bone sclerosis	2.0 ± 0.45	2.55 ± 0.52
Trabecular bone edema	1.55 ± 0.93	2.64 ± 0.92
Subchondral bone overgrowth	1.18 ± 0.87	1.09 ± 0.70
Composite MRI score	9.18 ± 3.12	11.64 ± 2.80

*A lower score is better.

TABLE VIII MRI Scores for Fill of Chondral Defect*

	Mean Score ± SD *(points)*	
	APEF	APEF+BMDMSCs
Amount of defect fill	3.45 ± 0.69	3.55 ± 0.69
Character of defect fill	2.91 ± 0.54	2.73 ± 0.65
Interface of defect	3.18 ± 0.87	2.73 ± 0.79
Composite score	9.55 ± 1.81	9.0 ± 1.67

*A higher score is better.

five regions (central and peripheral repair sites and host sites adjacent to, near to, and far from the repair). Fifteen sites were tested per sample (Fig. 1-C). At each site, rapid indentation tests were performed for one second to a depth of 100 μm using a 0.8-mm-diameter sphere-ended indenter attached to a Mach-1 V500cs mechanical testing system (Biomomentum). Structural stiffness (in N/mm) was calculated as the peak load normalized to the applied 10-μm indentation displacement.

Micro-CT of Tissue Thickness and Fixed Charge Density

Structural and physiological image data were obtained with micro-CT. Structural micro-CT images were obtained with a SkyScan 1076 scanner with an isotropic voxel size[24] $(36\ \mu m)^3$, by applying an electrical potential of 100 kVp and a current of 100 μA, and using a 0.038-mm copper plus 0.5-mm aluminum filter. From these scans, cartilaginous tissue thickness was determined for each of the fifteen test sites on each trochlear ridge[25]. Sagittal and transaxial slices, aligned with the test positions, were thresholded to determine the two interfaces among air, cartilaginous tissue, and calcified tissue. Material stiffness (in MPa) was then calculated as stress (peak load normalized to cross-sectional area of the indenter) relative to strain (displacement normalized to cartilaginous thickness).

Physiological Hexabrix (ioxaglate meglumine and ioxaglate sodium; Guerbet)-enhanced micro-CT scans were then performed after equilibration with 20% Hexabrix in phosphate-buffered saline solution (PBS). From these scans, an index of tissue fixed charge density was determined for each site[24,26].

Histological Analysis

Cartilaginous repair tissue was analyzed histologically. Transaxial blocks were prepared to include the lesion sites and the far host sites, decalcified in 10% ethylenediaminetetraacetic acid (EDTA), embedded in paraffin, and stained with hematoxylin and eosin or safranin O. All histological sections were graded according to the modified O'Driscoll scoring system (Table IV) as previously described[27].

Statistical Analysis

To determine the effects of BMDMSCs, paired t tests were performed on data (APEF alone versus APEF+BMDMSCs) at each region (far, near, and adjacent host sites as well as peripheral and central repair sites). To determine the overall independent and interactive effects of treatment (APEF alone versus APEF+BMDMSCs) and region (far, near, and adjacent host sites as well as peripheral and central repair sites), data were analyzed by two-way repeated-measures analysis of variance (ANOVA). Scores derived from the arthroscopic, histological, MRI, and biomechanical evaluations were compared using the Wilcoxon signed rank analyses with significance set at $p < 0.05$. All analyses

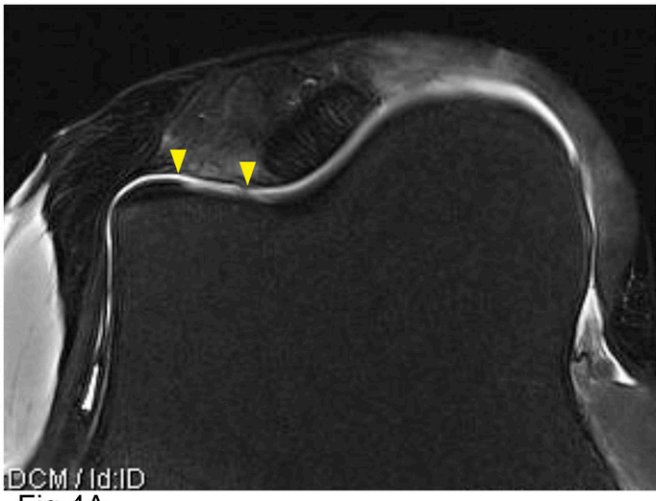

Fig 4A

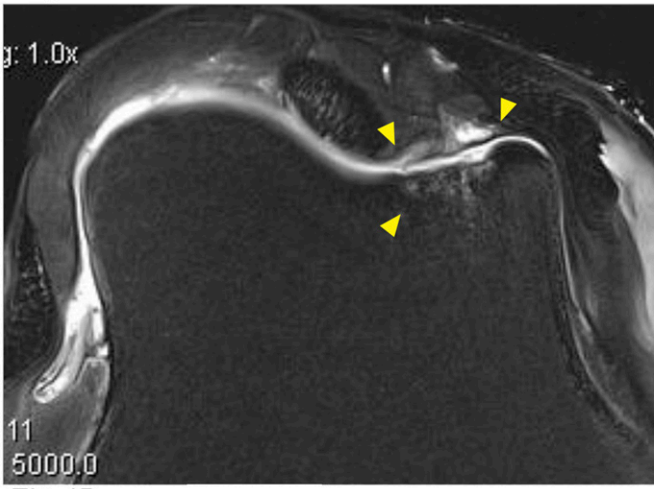

Fig 4B

Fig. 4

Proton density of fat-saturated axial plane MRIs of lateral trochlear ridges treated with APEF (**Fig. 4-A**) or APEF+BMDMSCs (**Fig. 4-B**). The down-pointing arrowheads indicate the periphery of the defects, and the arrowhead pointing up in **Figure 4-B** indicates decreased subchondral bone density as well as subchondral and trabecular bone fluid/edema.

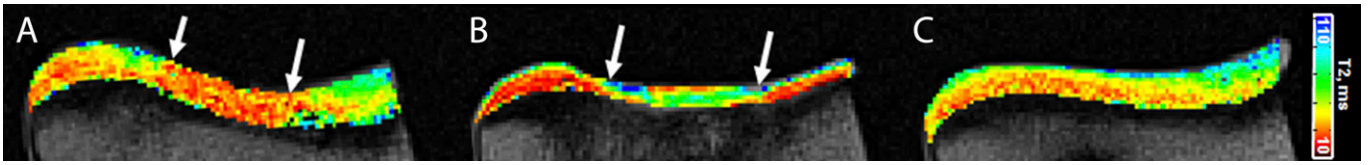

Fig. 5

MRI T2 maps demonstrating differences in articular cartilage matrix organization and composition in the repair regions in the APEF (**Fig. 5-A**) and APEF+BMDMSCs (**Fig. 5-B**) groups compared with native control cartilage (**Fig. 5-C**). The arrows indicate the margins of the repair zones. Both defects lack the laminar pattern typical of the native cartilage, in which the T2 values increase from low (red/orange) values at the bone-cartilage interface to higher (green/blue) values at the articular surface. The repair treated with APEF+BMDMSCs (**Fig. 5-B**) has thinner repair tissue and higher T2 values (suggestive of greater water content) than the repair treated only with APEF (**Fig. 5-A**).

were performed with and without the horses in which bone formed within the defects.

Source of Funding

Funding was provided by grants RC2 AR058929 (C.R.C., L.R.G., and R.L.S.), 1K08AR054903-01A2 (L.R.G. and C.W.M.), R01 AR051963 (C.R.C.), and R01 AR044058 and P01 AG007996 (R.L.S.) from the National Institutes of Health (NIH), which did not participate in the investigation; the Albert Ferguson Endowed Chair (C.R.C.) at the University of Pittsburgh; and the Barbara Cox Anthony University Endowed Chair (C.W.M.) at Colorado State University. DSM Biomedical supplied the custom coring tools that were used to create the chondral defects.

Results

Arthroscopic Defect Creation and Scoring

All surgical defects were consistent in size, shape, location, and depth. Within five to seven minutes following implantation, the filling was even with the surrounding cartilage. Three-month follow-up arthroscopic evaluations revealed all defects to be filled with repair tissue and to have a smooth or smooth-to-cobblestone surface appearance, with firm attachment to the underlying subchondral bone and surrounding cartilage. None of the defects had exposed subchondral bone. The overall International Cartilage Repair Society (ICRS) scores derived with the three-month arthroscopic examination ranged from 5 to 11 with an average (and standard deviation [SD]) of 8.4 ± 1.9 for the APEF group and 7 to 12 (10.4 ± 1.59) for the APEF+BMDMSCs group (Table V), which were not significantly different ($p = 1.0$). At twelve months, the repair tissue was more mottled and varied from smooth and fibrous to a cobblestone appearance. Composite ICRS scores at twelve months were 8.2 ± 2.1 for the APEF group and 8.3 ± 1.5 for the APEF+BMDMSCs group (Table V), which were not significantly different ($p = 0.87$).

Histological Analysis

Twenty-three of the twenty-four chondral defects had fair-to-good fill (with the APEF or APEF+BMDMSCs) and integration with the surrounding cartilage (Fig. 2). Repairs in general had a cellular appearance at the base of the defect with positive staining for glycosaminoglycan (GAG). The middle-to-superficial part of the repair had a more fibrous, hypocellular appearance with an absence of GAG staining. Cumulative and subcategory histological scores did not differ significantly between the APEF and APEF+BMDMSCs groups (Table VI).

Bone formed within four of the twelve defects repaired with APEF+BMDMSCs (Fig. 3) but in none of those repaired with APEF alone. Bone formation within the defects appeared to be separate from the underlying bone and did not seem to be advancement of the subchondral bone. The repair tissue that formed bone still showed GAG accumulation within and integration to the surrounding cartilage. However, integration of the repair tissue with the subchondral bone was poor in three of the four defects.

MRI Analysis

MRI of the defects revealed no statistically significant difference in cumulative scores between the two groups (Tables VII and VIII). Subcategory scores analyzed separately revealed a significantly greater amount of trabecular bone edema in the defects repaired with APEF+BMDMSCs compared with defects repaired with APEF alone (Fig. 4).

T2 Mapping of Defects

Four of the defects (all repaired with APEF+BMDMSCs) demonstrated development of bone-like tissue in the repair zones. These defects and those in the paired contralateral limbs were excluded from the T2 analysis. No significant difference in mean T2 values in the repair tissue was detected between the APEF and APEF+BMDMSC-treated defects in the remaining eight horses (Wilcoxon signed rank test, $p = 0.24$) (Fig. 5).

Cartilaginous Tissue Thickness

Inclusion of BMDMSCs led to less cartilaginous tissue thickness (Fig. 6-A) in the central repair site (−24%, $p < 0.05$) and a tendency for less thickness in the peripheral repair site (−16%, $p = 0.07$), but no detectable difference in the adjacent, near, or far host regions (each $p > 0.1$). Overall, the cartilaginous tissue thickness varied with region ($p < 0.001$) but not treatment ($p = 0.11$). The thickness of the cartilaginous tissue was highest at the far host region, 22% thinner at the near host region, and 26% to 28% thinner at the central and peripheral repair regions.

Cartilaginous Tissue Composition—Fixed Charge Density

Inclusion of BMDMSCs did not affect Hexabrix-enhanced micro-CT values (Fig. 6-B) in any region (each $p > 0.4$). Overall, Hexabrix-enhanced micro-CT values varied with

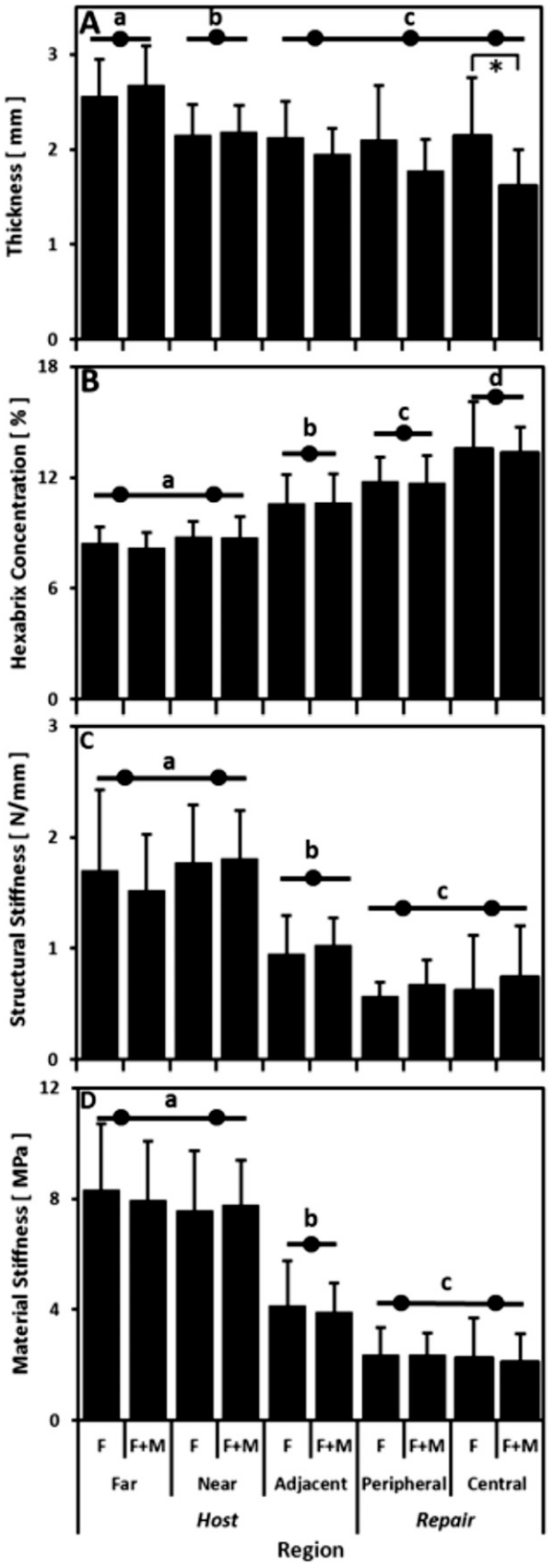

Fig. 6

Thickness (**Fig. 6-A**), Hexabrix concentration (**Fig. 6-B**), structural stiffness (**Fig. 6-C**), and material stiffness (**Fig. 6-D**) of host and repair tissue in the APEF (F) and the APEF+BMDMSCs (F+M)-treated trochleae. Data are given as the mean ± SD (n = 12). For comparisons of the five regions (far, near, and adjacent host sites and peripheral and central repair sites), the bars under each horizontal line represent values that do not differ significantly from one another. The horizontal lines with different lowercase letters indicate that the groups differ from one another. * = $p < 0.05$ according to the t test.

region ($p < 0.001$) but not treatment ($p = 0.78$), and there were no interactive effects ($p = 0.99$).

Cartilaginous Tissue Stiffness

The structural stiffness of the cartilaginous tissue was not detectably affected by the inclusion of BMDMSCs (Fig. 6-C), in either the central repair (+19%, $p = 0.19$) or other regions (each $p > 0.26$). Overall, structural stiffness varied substantially with region ($p < 0.001$) but not treatment ($p = 0.72$), and there were no interactive effects ($p = 0.32$).

Material stiffness also was not affected by the inclusion of BMDMSCs (Fig. 6-D) in any region (each $p > 0.48$). Overall, material stiffness varied substantially with region ($p < 0.001$) but not treatment ($p = 0.74$), and there were no interactive effects ($p = 0.92$).

Discussion

APEF, both alone and with BMDMSCs, supported the formation of repair tissue within critical-size full-thickness cartilage defects, with some deterioration between three and twelve months. Arthroscopic evaluation at three months revealed tissue that appeared intact on the edges with a smooth-to-cobblestone appearance and fair-to-good integration to the subchondral bone as determined by arthroscopic probing. At twelve months, the repair tissue in both treatment groups grossly appeared less smooth (more undulating surfaces) and had slightly less integration with the surrounding cartilage and underlying bone as evidenced by softer superficial surface tissue when probed. Deterioration of cartilage repair over time was consistent with the findings in other studies of cartilage healing[9,20,28]. This highlights the importance of extending cartilage repair studies beyond three to six months since, as tissue continues to progress through stages of healing, degenerative processes change the nature of the repair tissue.

The histological appearance of the repair tissue at twelve months was generally fibrous in nature. Safranin-O staining of GAG was mainly close to the subchondral bone, a finding that was similar to observations in other cartilage-healing studies in which biologics were placed in osteochondral defects[9,20,27-29]. Regardless of treatment, the integration of all defects with the surrounding tissue appeared to be intact, although the transition zone from the surrounding cartilage of the defect to the repair tissue was easily detectable. Subchondral bone attachment appeared good for most defects, with some having specific areas of poor integration.

The development of bone in four of the twelve defects repaired with APEF+BMDMSCs was surprising and was not reported in previous studies in which BMDMSCs were combined with fibrin or fibrin and platelet-rich plasma[4,9,30]. Growth factors in platelet-rich plasma can be beneficial to cartilage health[15,31-33]. In the present study, APEF alone appeared to support formation of cartilage-like repair tissue with good integration to the surrounding cartilage, GAG in the base of the defect, and no bone formation, which is consistent with the findings in other chondral defect models in which APEF was used[32,34,35]. While platelet-rich plasma can support chondrogenesis, it can also promote osteogenesis, as has been shown in bone-healing studies. This suggests that the BMDMSCs within the APEF were signaled to undergo osteogenesis[36-38]. A study by Perut et al. revealed that greater leukocyte counts in platelet concentrate increased the concentrate's potential to promote osteogenesis of bone marrow stromal cells[36]. The APEF used in the current study did not contain white blood cells, so the growth factor milieu from the platelets may have promoted osteogenesis of the BMDMSCs in the defects in which bone formed. Lastly, BMDMSCs in this study were not evaluated for osteogenesis at the end of expansion cultures as we did not anticipate bone formation; this may be something to test in the future.

The APEF preparation method may have affected the results. Previous studies have shown that the release of bioactive substances and cellular migration from fibrin gels is affected by fibrin concentration[19,39,40]. On the basis of that work, we performed a pilot study (not shown), prior to this investigation, in which we diluted the APEF as much as possible to encourage cell migration[19] while retaining sufficient fibrin to effect bonding to both the underlying bone and the surrounding cartilage. Alternatively, diluted APEF could be placed under a membrane in a manner similar to autologous chondrocyte implantation[41]; however, such an additional procedure adds time, and possibly morbidity, to the procedure[42]. In a similar study to ours, Wilke et al. reported enhanced healing at one month when culture-expanded BMDMSCs had been added to a fibrin matrix in an osteochondral defect model in horses[9] but no benefits to chondral repair at eight months. In that study, bone was not found in the repair tissue, which further suggests that the platelets induced osteogenesis of the implanted BMDMSCs in our study. Similar to Wilke et al., we did not find a long-term benefit of BMDMSCs in terms of cartilage repair beyond what was achieved with fibrin alone. The fact that Wilke et al. did not observe bone formation in their BMDMSC group and we did might be explained by the difference in the times that the animals were euthanized (at eight months in their study and at twelve months in ours). It is possible that bone formation is a late response. A more recent study by Frisbie et al.[43] comparing a fibrin scaffold to fibrin with the addition of autologous or allogenic chondrocytes showed improved repair tissues in the group treated with fibrin and autologous chondrocytes. This information suggests that the observed bone formation in the APEF+BMDMSCs group in the current study may be evidence of a BMDMSC response to osteogenic signaling from the growth factor milieu released by the platelets.

The MRI, T2 mapping, and biomechanical findings in our study were reflective of the histological findings. No differences between treatment groups were seen with respect to the MRI scores for defect fill, character, or integration. The increase in trabecular bone edema in the defects repaired with APEF+BMDMSCs may have been related to the tendency for bone formation in the repair tissue, and has not been reported previously to our knowledge. T2 mapping of the repair tissue of both treatment groups revealed differences between the repair tissue and the native cartilage, including a lack of the laminar pattern typical of native tissue along with the softer biomechanical properties. These changes are typical of those reported in studies of osteochondral defects repaired with various biological implants[8,44].

Micro-CT and Hexabrix-enhanced micro-CT findings were also indicative of the histological results. High Hexabrix concentrations in the defects of both treatment groups indicated a proteoglycan content lower than that of normal articular cartilage. This was consistent with the histochemical findings and well as with the decreased structural and material stiffness within the lesion compared with the control articular cartilage. Micro-CT analysis also revealed that, in the defects repaired with APEF alone, the repair tissue was thicker and more closely approximated the thickness of the control cartilage than the lesions repaired with APEF+BMDMSCs. This indicates the continuing need to fully regenerate cartilage, to its original histological properties but also to its biomechanical stiffness and thickness. This is likely needed for long-term integrity under the typical loading associated with the joint environment[45].

Currently, the trend in biologic osteochondral repair is to "simplify" the procedure by (1) eliminating the need for two procedures, (2) utilizing a scaffold that does not require suturing a membrane over the defect, and (3) eliminating the need for and associated regulatory implications of a culture-expanded cell population[41,46]. Although the defects treated with APEF alone in this study did not reveal a regenerated repair tissue, the APEF alone appeared to support the formation of chondral-like repair tissue since tissue was integrated to the surrounding cartilage, and in many cases the subchondral bone, and also frequently had GAG formation in the base of the defect. Furthermore, the thickness of the repair tissue more closely approximated the surrounding cartilage. A scaffold with platelets alone and an absence of cells may bring important growth factors to chondral defects and enhance repair, and many groups are currently investigating this possibility[47-50].

In summary, this work showed that the addition of BMDMSCs to APEF did not improve chondral repair and in fact may support ectopic bone formation. Instead, APEF alone appeared to support the formation of chondral repair tissue. Future work will determine if use of platelets alone in scaffolds is superior to techniques such as microfracture, autologous chondrocyte implantation, or osteochondral implantation.

Appendix

eA An expanded Materials and Methods section is available with the online version of this article as a data supplement at jbjs.org. ■

NOTE: The authors thank Dr. Dora Ferris, Dr. Valerie Moorman, and Ms. Jennifer Suddreth for their care of the horses in this study; Ms. Meaghan Monahan for her help with manuscript preparation; Mr. Daniel Arnold and Mr. David Berry for their help with the biomechanical studies and imaging; and Dr. Christian Coyle, Dr. Megan Bowers, and Kimberly Rankin for their help organizing imaging, arthroscopy, and specimen preparation at the University of Pittsburgh.

Laurie R. Goodrich, DVM, PhD[1]
John D. Kisiday, PhD[1]
Paul S. Morley, DVM, PhD[1]
C. Wayne McIlwraith, BVSc, PhD, DSc, FRCVS[1]
Albert C. Chen, PhD[2]
Alvin W. Su, MD, PhD[2]
Esther Cory, MA[2]
Robert L. Sah, MD, ScD[2]
Natasha M. Werpy, DVM[3]
Ashley A. Williams, MS[4]
Constance R. Chu, MD[4]

[1]Gail Holmes Equine Orthopedic Research Center, Colorado State University, 300 West Drake Road, Fort Collins, CO 80523

[2]Department of Bioengineering, Mail Code 0412, University of California, San Diego, 9500 Gilman Drive, La Jolla, CA 92093-0412

[3]Large Animal Clinical Sciences, 2015 S.W. 16th Avenue, Gainesville, FL 32608

[4]Department of Orthopedic Surgery, Stanford University School of Medicine, 450 Broadway Street, Redwood City, CA 94063.

E-mail address for C.R. Chu: chucr@stanford.edu

References

1. Wakitani S, Goto T, Pineda SJ, Young RG, Mansour JM, Caplan AI, Goldberg VM. Mesenchymal cell-based repair of large, full-thickness defects of articular cartilage. J Bone Joint Surg Am. 1994 Apr;76(4):579-92.

2. McIlwraith CW, Frisbie DD, Rodkey WG, Kisiday JD, Werpy NM, Kawcak CE, Steadman JR. Evaluation of intra-articular mesenchymal stem cells to augment healing of microfractured chondral defects. Arthroscopy. 2011 Nov;27(11):1552-61. Epub 2011 Aug 20.

3. Centeno CJ, Busse D, Kisiday J, Keohan C, Freeman M, Karli D. Increased knee cartilage volume in degenerative joint disease using percutaneously implanted, autologous mesenchymal stem cells. Pain Physician. 2008 May-Jun;11(3):343-53.

4. Haleem AM, Singergy AA, Sabry D, Atta HM, Rashed LA, Chu CR, El Shewy MT, Azzam A, Abdel Aziz MT. The clinical use of human culture-expanded autologous bone marrow mesenchymal stem cells transplanted on platelet-rich fibrin glue in the treatment of articular cartilage defects: a pilot study and preliminary results. Cartilage. 2010 Oct;1(4):253-61.

5. Giannini S, Buda R, Battaglia M, Cavallo M, Ruffilli A, Ramponi L, Pagliazzi G, Vannini F. One-step repair in talar osteochondral lesions: 4-year clinical results and T2-mapping capability in outcome prediction. Am J Sports Med. 2013 Mar; 41(3):511-8. Epub 2012 Dec 5.

6. Centeno CJ, Schultz JR, Cheever M, Freeman M, Faulkner S, Robinson B, Hanson R. Safety and complications reporting update on the re-implantation of culture-expanded mesenchymal stem cells using autologous platelet lysate technique. Curr Stem Cell Res Ther. 2011 Dec;6(4):368-78.

7. Wakitani S, Okabe T, Horibe S, Mitsuoka T, Saito M, Koyama T, Nawata M, Tensho K, Kato H, Uematsu K, Kuroda R, Kurosaka M, Yoshiya S, Hattori K, Ohgushi H. Safety of autologous bone marrow-derived mesenchymal stem cell transplantation for cartilage repair in 41 patients with 45 joints followed for up to 11 years and 5 months. J Tissue Eng Regen Med. 2011 Feb;5(2):146-50.

8. Fortier LA, Potter HG, Rickey EJ, Schnabel LV, Foo LF, Chong LR, Stokol T, Cheetham J, Nixon AJ. Concentrated bone marrow aspirate improves full-thickness cartilage repair compared with microfracture in the equine model. J Bone Joint Surg Am. 2010 Aug 18;92(10):1927-37.

9. Wilke MM, Nydam DV, Nixon AJ. Enhanced early chondrogenesis in articular defects following arthroscopic mesenchymal stem cell implantation in an equine model. J Orthop Res. 2007 Jul;25(7):913-25.

10. Hui TY, Cheung KM, Cheung WL, Chan D, Chan BP. In vitro chondrogenic differentiation of human mesenchymal stem cells in collagen microspheres: influence of cell seeding density and collagen concentration. Biomaterials. 2008 Aug; 29(22):3201-12. Epub 2008 May 7.

11. Pastides P, Chimutengwende-Gordon M, Maffulli N, Khan W. Stem cell therapy for human cartilage defects: a systematic review. Osteoarthritis Cartilage. 2013 May;21(5):646-54. Epub 2013 Feb 26.

12. van Buul GM, Koevoet WLM, Kops N, Bos PK, Verhaar JA, Weinans H, Bernsen MR, van Osch GJ. Platelet-rich plasma releasate inhibits inflammatory processes in osteoarthritic chondrocytes. Am J Sports Med. 2011 Nov;39(11):2362-70. Epub 2011 Aug 19.

13. Lacci KM, Dardik A. Platelet-rich plasma: support for its use in wound healing. Yale J Biol Med. 2010 Mar;83(1):1-9.

14. Pagnotto MR, Wang Z, Karpie JC, Ferretti M, Xiao X, Chu CR. Adeno-associated viral gene transfer of transforming growth factor-beta1 to human mesenchymal stem cells improves cartilage repair. Gene Ther. 2007 May;14(10):804-13. Epub 2007 Mar 8.

15. Smyth NA, Murawski CD, Fortier LA, Cole BJ, Kennedy JG. Platelet-rich plasma in the pathologic processes of cartilage: review of basic science evidence. Arthroscopy. 2013 Aug;29(8):1399-409. Epub 2013 May 11.

16. Giannini S, Buda R, Cavallo M, Ruffilli A, Cenacchi A, Cavallo C, Vannini F. Cartilage repair evolution in post-traumatic osteochondral lesions of the talus: from open field autologous chondrocyte to bone-marrow-derived cells transplantation. Injury. 2010 Nov;41(11):1196-203. Epub 2010 Oct 8.

17. Buda R, Vannini F, Cavallo M, Grigolo B, Cenacchi A, Giannini S. Osteochondral lesions of the knee: a new one-step repair technique with bone-marrow-derived cells. J Bone Joint Surg Am. 2010 Dec;92(Suppl 2):2-11.

18. Kisiday JD, Goodrich LR, McIlwraith CW, Frisbie DD. Effects of equine bone marrow aspirate volume on isolation, proliferation, and differentiation potential of mesenchymal stem cells. Am J Vet Res. 2013 May;74(5):801-7.

19. Hale BW, Goodrich LR, Frisbie DD, McIlwraith CW, Kisiday JD. Effect of scaffold dilution on migration of mesenchymal stem cells from fibrin hydrogels. Am J Vet Res. 2012 Feb;73(2):313-8.

20. Goodrich LR, Hidaka C, Robbins PD, Evans CH, Nixon AJ. Genetic modification of chondrocytes with insulin-like growth factor-1 enhances cartilage healing in an equine model. J Bone Joint Surg Br. 2007 May;89(5):672-85.

21. Xu X, Shi D, Shen Y, Xu Z, Dai J, Chen D, Teng H, Jiang Q. Full-thickness cartilage defects are repaired via a microfracture technique and intraarticular injection of the small-molecule compound kartogenin. Arthritis Res Ther. 2015;17:20. Epub 2015 Feb 2.

22. Nieminen MT, Rieppo J, Töyräs J, Hakumäki JM, Silvennoinen J, Hyttinen MM, Helminen HJ, Jurvelin JS. T2 relaxation reveals spatial collagen architecture in articular cartilage: a comparative quantitative MRI and polarized light microscopic study. Magn Reson Med. 2001 Sep;46(3):487-93.

23. Miller RE, Grodzinsky AJ, Barrett MF, Hung HH, Frank EH, Werpy NM, McIlwraith CW, Frisbie DD. Effects of the combination of microfracture and self-assembling peptide filling on the repair of a clinically relevant trochlear defect in an equine model. J Bone Joint Surg Am. 2014 Oct 1;96(19):1601-9.

24. Pallante AL, Görtz S, Chen AC, Healey RM, Chase DC, Ball ST, Amiel D, Sah RL, Bugbee WD. Treatment of articular cartilage defects in the goat with frozen versus fresh osteochondral allografts: effects on cartilage stiffness, zonal composition, and structure at six months. J Bone Joint Surg Am. 2012 Nov 7;94(21):1984-95.

25. Chan EF, Liu IL, Semler EJ, Aberman HM, Simon TM, Chen AC, Truncale KG, Sah RL. Association of 3-dimensional cartilage and bone structure with articular cartilage properties in and adjacent to autologous osteochondral grafts after 6 and 12 months in a goat model. Cartilage. 2012 Jul 1;3(3).

26. Palmer AW, Guldberg RE, Levenston ME. Analysis of cartilage matrix fixed charge density and three-dimensional morphology via contrast-enhanced

microcomputed tomography. Proc Natl Acad Sci U S A. 2006 Dec 19;103 (51):19255-60. Epub 2006 Dec 8.

27. Frisbie DD, Lu Y, Kawcak CE, DiCarlo EF, Binette F, McIlwraith CW. In vivo evaluation of autologous cartilage fragment-loaded scaffolds implanted into equine articular defects and compared with autologous chondrocyte implantation. Am J Sports Med. 2009 Nov;37(Suppl 1):71S-80S.

28. Hidaka C, Goodrich LR, Chen CT, Warren RF, Crystal RG, Nixon AJ. Acceleration of cartilage repair by genetically modified chondrocytes over expressing bone morphogenetic protein-7. J Orthop Res. 2003 Jul;21(4):573-83.

29. Frisbie DD, Bowman SM, Colhoun HA, DiCarlo EF, Kawcak CE, McIlwraith CW. Evaluation of autologous chondrocyte transplantation via a collagen membrane in equine articular defects: results at 12 and 18 months. Osteoarthritis Cartilage. 2008 Jun;16(6):667-79. Epub 2007 Nov 26.

30. Lee JC, Min HJ, Park HJ, Lee S, Seong SC, Lee MC. Synovial membrane-derived mesenchymal stem cells supported by platelet-rich plasma can repair osteochondral defects in a rabbit model. Arthroscopy. 2013 Jun;29(6):1034-46.

31. Park SI, Lee HR, Kim S, Ahn MW, Do SH. Time-sequential modulation in expression of growth factors from platelet-rich plasma (PRP) on the chondrocyte cultures. Mol Cell Biochem. 2012 Feb;361(1-2):9-17. Epub 2011 Sep 29.

32. Milano G, Deriu L, Sanna Passino E, Masala G, Manunta A, Postacchini R, Saccomanno MF, Fabbriciani C. Repeated platelet concentrate injections enhance reparative response of microfractures in the treatment of chondral defects of the knee: an experimental study in an animal model. Arthroscopy. 2012 May;28(5):688-701. Epub 2012 Jan 25.

33. Lee HR, Park KM, Joung YK, Park KD, Do SH. Platelet-rich plasma loaded hydrogel scaffold enhances chondrogenic differentiation and maturation with up-regulation of CB1 and CB2. J Control Release. 2012 May 10;159(3):332-7. Epub 2012 Feb 15.

34. Sun Y, Feng Y, Zhang CQ, Chen SB, Cheng XG. The regenerative effect of platelet-rich plasma on healing in large osteochondral defects. Int Orthop. 2010 Apr;34(4):589-97. Epub 2009 May 12.

35. Qi YY, Chen X, Jiang YZ, Cai HX, Wang LL, Song XH, Zou XH, Ouyang HW. Local delivery of autologous platelet in collagen matrix simulated in situ articular cartilage repair. Cell Transplant. 2009;18(10):1161-9. Epub 2009 Aug 5.

36. Perut F, Filardo G, Mariani E, Cenacchi A, Pratelli L, Devescovi V, Kon E, Marcacci M, Facchini A, Baldini N, Granchi D. Preparation method and growth factor content of platelet concentrate influence the osteogenic differentiation of bone marrow stromal cells. Cytotherapy. 2013 Jul;15(7):830-9.

37. Ronca A, Guarino V, Raucci MG, Salamanna F, Martini L, Zeppetelli S, Fini M, Kon E, Filardo G, Marcacci M, Ambrosio L. Large defect-tailored composite scaffolds for in vivo bone regeneration. J Biomater Appl. 2014 Nov;29(5):715-27. Epub 2014 Jun 20.

38. Lee DH, Ryu KJ, Kim JW, Kang KC, Choi YR. Bone marrow aspirate concentrate and platelet-rich plasma enhanced bone healing in distraction osteogenesis of the tibia. Clin Orthop Relat Res. 2014 Dec;472(12):3789-97.

39. Stolzing A, Colley H, Scutt A. Effect of age and diabetes on the response of mesenchymal progenitor cells to fibrin matrices. Int J Biomater. 2011;2011: 378034-42. Epub 2011 Dec 13.

40. Lee HH, Haleem AM, Yao V, Li J, Xiao X, Chu CR. Release of bioactive adeno-associated virus from fibrin scaffolds: effects of fibrin glue concentrations. Tissue Eng Part A. 2011 Aug;17(15-16):1969-78. Epub 2011 May 11.

41. Fritz J, Janssen P, Gaissmaier C, Schewe B, Weise K. Articular cartilage defects in the knee—basics, therapies and results. Injury. 2008 Apr;39(Suppl 1):S50-7.

42. Ahmed TAE, Hincke MT. Strategies for articular cartilage lesion repair and functional restoration. Tissue Eng Part B Rev. 2010 Jun;16(3):305-29.

43. Frisbie DD, McCarthy HE, Archer CW, Barrett MF, McIlwraith CW. Evaluation of articular cartilage progenitor cells for the repair of articular defects in an equine model. J Bone Joint Surg Am. 2015 Mar 18;97(6):484-93.

44. Gelber PE, Batista J, Millan-Billi A, Patthauer L, Vera S, Gomez-Masdeu M, Monllau JC. Magnetic resonance evaluation of TruFit® plugs for the treatment of osteochondral lesions of the knee shows the poor characteristics of the repair tissue. Knee. 2014 Aug;21(4):827-32. Epub 2014 May 9.

45. McMahon LA, O'Brien FJ, Prendergast PJ. Biomechanics and mechanobiology in osteochondral tissues. Regen Med. 2008 Sep;3(5):743-59.

46. Moran CJ, Pascual-Garrido C, Chubinskaya S, Potter HG, Warren RF, Cole BJ, Rodeo SA. Restoration of articular cartilage. J Bone Joint Surg Am. 2014 Feb 19;96(4):336-44.

47. Perdisa F, Filardo G, Di Matteo B, Marcacci M, Kon E. Platelet rich plasma: a valid augmentation for cartilage scaffolds? A systematic review. Histol Histopathol. 2014 Jul;29(7):805-14. Epub 2014 Jan 24.

48. Dold AP, Zywiel MG, Taylor DW, Dwyer T, Theodoropoulos J. Platelet-rich plasma in the management of articular cartilage pathology: a systematic review. Clin J Sport Med. 2014 Jan;24(1):31-43.

49. Tadie J, Ann X. Comments on "Repeated platelet concentrate injections enhance reparative response of microfractures in the treatment of chondral defects of the knee: an experimental study in an animal model" by Milano et al. Arthroscopy. 2013 Oct;29(10):1599.

50. Siclari A, Mascaro G, Gentili C, Kaps C, Cancedda R, Boux E. Cartilage repair in the knee with subchondral drilling augmented with a platelet-rich plasma-immersed polymer-based implant. Knee Surg Sports Traumatol Arthrosc. 2014 Jun;22(6):1225-34. Epub 2013 Apr 7.